

## Article

# Application of a TEMPO-Polypyrrole Polymer for NO<sub>x</sub>-Mediated Oxygen Electroreduction

Daniil A. Lukyanov <sup>1</sup>, Arseniy Y. Kalnin <sup>1,2</sup>, Lyubov G. Rubicheva <sup>3</sup>, Vasiliy V. Potapenkov <sup>1</sup>, Olga Y. Bakulina <sup>1,2</sup> and Oleg V. Levin <sup>1,2,\*</sup>

<sup>1</sup> Institute of Chemistry, Saint Petersburg University, 7/9 Universitetskaya Nab., 199034 St. Petersburg, Russia

<sup>2</sup> Sirius University of Science and Technology, 1 Olympic Ave., 354340 Sochi, Russia

<sup>3</sup> Institute of Organic Chemistry, Faculty of Chemistry, University of Vienna, Währinger Str. 38, 1090 Vienna, Austria

\* Correspondence: o.levin@spbu.ru

**Abstract:** The oxygen reduction reaction (ORR) is one of the key processes for electrochemical energy storage, such as the cathode process in fuel cells and metal–air batteries. To date, the efficiency of the ORR half-reaction limits the overall performance of these energy storage devices. Traditional platinum-based materials are expensive and cannot provide the desired ORR efficiency. As an alternative, a new catalytic scheme for an ORR was proposed, which consisted of an electrode modified with a TEMPO-containing conductive polymer and a solution redox mediator system based on nitrogen oxides (NO<sub>x</sub>). NO<sub>x</sub> is perfect for oxygen reduction in solution, which, however, cannot be efficiently reduced onto a pristine electrode, while TEMPO is inactive in the ORR itself but catalyzes the electrochemical reduction of NO<sub>2</sub> on the electrode surface. Together, these catalysts have a synergistic effect, enabling an efficient ORR in an acidic medium. In the present study, the synthesis of a novel TEMPO-containing conductive polymer and its application in the synergistic ORR system with a NO<sub>x</sub> mediator is described. The proposed mediator system may increase the performance of proton-exchange fuel cells and metal–air batteries.

**Keywords:** TEMPO; ORR; redox mediators; NO<sub>x</sub>; fuel cells



**Citation:** Lukyanov, D.A.; Kalnin, A.Y.; Rubicheva, L.G.; Potapenkov, V.V.; Bakulina, O.Y.; Levin, O.V. Application of a TEMPO-Polypyrrole Polymer for NO<sub>x</sub>-Mediated Oxygen Electroreduction. *Catalysts* **2022**, *12*, 1466. <https://doi.org/10.3390/catal12111466>

Academic Editor: Ji Qi

Received: 3 October 2022

Accepted: 17 November 2022

Published: 18 November 2022

**Publisher's Note:** MDPI stays neutral with regard to jurisdictional claims in published maps and institutional affiliations.



**Copyright:** © 2022 by the authors. Licensee MDPI, Basel, Switzerland. This article is an open access article distributed under the terms and conditions of the Creative Commons Attribution (CC BY) license (<https://creativecommons.org/licenses/by/4.0/>).

## 1. Introduction

The electrochemical four-electron oxygen reduction reaction (ORR) comprises the cathodic process in fuel cells and metal–air batteries and is becoming one of the most important electrochemical reactions for energy storage and conversion [1]. The dioxygen molecule, in terms of thermodynamics, is one of the most powerful oxidants (Table 1), but the great stability of the double O=O bond results in a low reactivity of the oxygen [2]. In particular, due to its sluggish kinetics, the electrochemical reduction of the dioxygen molecule requires an efficient redox catalyst which transfers electrons from the electrode to the O<sub>2</sub> molecule [3]. An ORR catalyst for energy storage applications should also possess high selectivity for the four-electron ORR over the adverse process of two-electron oxygen reduction to peroxides, which decreases the half-cell potential of the cathode and leads to the accumulation of hazardous peroxide products (Table 1, Equation (2)) [4–6].

Commercial ORR cathode materials are based on precious metals, mostly Pt, due to their catalytic activity and four-electron selectivity in the ORR reaction [7,8]. Platinum catalysts have high cost and low stability. Therefore, decreasing the use of platinum or replacing it in cathode catalysts is the main way for the development of new technologies for the commercial use of fuel cells [9–12]. The content of platinum in cathode materials can be reduced by using platinum alloys with other metals [13–16] or eliminated by using alternative catalytic systems, such as doped carbon nanomaterials [17–22]. The drawbacks of such catalysts are their tendency to agglomeration, uneven distribution of particles in polymer matrices, and washing out during operation, which deter the catalytic performance

of the materials [23–25]. Therefore, the development of effective ORR catalysts is a key scientific problem to be solved for fuel cell commercialization.

**Table 1.** Standard potentials of O<sub>2</sub>- and NO<sub>x</sub>- based half-reactions.

Nr.	Half-Reaction	E°, V	Ref.
1	$O_2 + 4 H^+ + 4 e^- \rightleftharpoons 2 H_2O$	1.229	[26]
2	$O_2 + 2 H^+ + 2 e^- \rightleftharpoons H_2O_2$	0.695	[26]
3	$HNO_2 + H^+ + e^- \rightleftharpoons NO\bullet_{(g)} + H_2O$	0.984	[26]
4	$NO_2\bullet_{(g)} + H^+ + e^- \rightleftharpoons HNO_2$	1.108	[26]
5	$NO_2\bullet_{(g)} + 2 H^+ + 2 e^- \rightleftharpoons NO\bullet_{(g)} + H_2O$	1.028 <sup>1</sup>	[26]
6	$TEMPO\bullet + H^+ + e^- \rightleftharpoons TEMPOH$	0.65	[27]
7	$TEMPO^+ + e^- \rightleftharpoons TEMPO\bullet$	0.745	[27]
8	$TEMPO^+ + H^+ + 2 e^- \rightleftharpoons TEMPOH$	0.70 <sup>2</sup>	[27]

<sup>1</sup> Calculated from Equations (3) and (4). <sup>2</sup> Calculated from Equations (6) and (7).

Nitrogen oxides (NO<sub>x</sub>) are considered promising mediators for the oxygen reduction reaction (ORR) [28–31]. The catalytic cycle of this mediator system in the electrochemical ORR is depicted in Figure 1a. NO, one of the components of the NO<sub>x</sub> system, efficiently reduces dioxygen, affording, through several intermediates, NO<sub>2</sub>, which can then be reduced back to NO. This process provides fast kinetics of oxygen reduction and is thermodynamically favored, with NO ΔE° of the reduction of O<sub>2</sub> by NO (Table 1, Equations (1) and (5)) of only 0.201 V, which means a high thermodynamic efficiency of the NO<sub>x</sub> mediator system in the ORR. The mediator cycle inherently produces H<sub>2</sub>O as a sole reduction product, which excludes the possibility of H<sub>2</sub>O<sub>2</sub> formation [32].

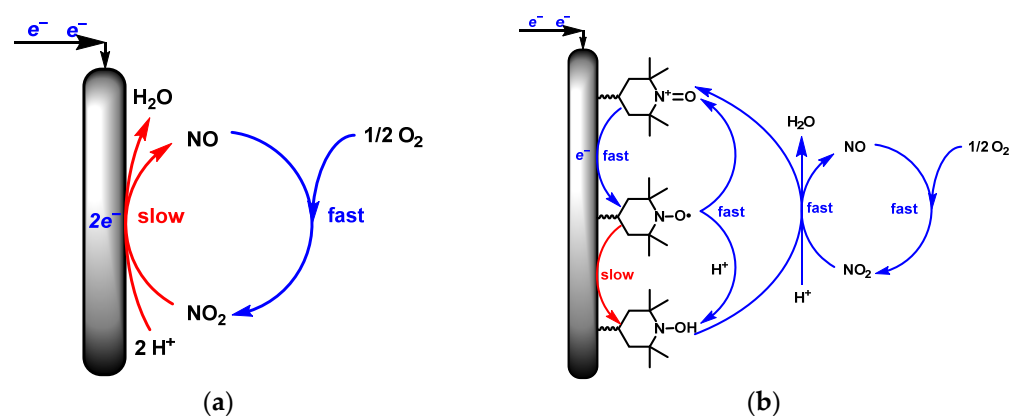


**Figure 1.** (a) Simplified catalytic cycle of NO<sub>x</sub>-mediated ORR and (b) generalized reaction scheme for NO<sub>x</sub>-mediated ORR on a TEMPO-modified electrode.

However, the electroreduction of NO<sub>2</sub> on the electrodes is limited by its poor kinetics and thus requires an additional catalytic system that will facilitate this process [32]. A possible solution to overcome this limitation is the use of an additional redox mediator, which can eliminate the kinetic limitations of electron transfer. An inorganic co-mediator system based on the VO<sup>2+</sup>/VO<sub>2</sub><sup>+</sup> couple was proposed for the NO<sub>x</sub> system; however, vanadyl itself showed poor reduction kinetics on the electrode [33,34]. Recently, aminoxyl derivatives, and, in particular, TEMPO, were proposed as dissolved co-mediators that facilitate the reduction of NO<sub>2</sub> and overcome this issue (Figure 1b) [35]. The standard potential of the TEMPO•/TEMPO<sup>+</sup> couple is 0.745 V (Table 1, Equation (7)), which is only 0.363 V lower than the NO<sub>2</sub> reduction potential (Table 1, Equation (4)). This co-mediator minimizes energy losses in this step, and, at the same time, ensures fast kinetics for both NO<sub>2</sub> reduction and electrode sites.

In our study, we propose an ORR catalytic system based on the  $\text{NO}_x$ -aminoxyl mediator system with a TEMPO catalyst immobilized on the surface of the electrode (Figure 1b) as a potential catalytic system for fuel cells and metal–air batteries. TEMPO radicals undergo disproportionation in an acid medium, producing an active reducing agent—TEMPO<sup>−</sup> anions—which rapidly reduces  $\text{NO}_2$  species to NO, forming TEMPO<sup>+</sup> cations, which can be easily electroreduced to neutral TEMPO species. The latter again produce TEMPO<sup>−</sup> species in an acid medium, and the mediator cycle continues. TEMPO fragments are bound on a conductive polymer backbone, which ensures a fast electron transport to the electrode surface, increasing the overall efficiency of the ORR. Such an architecture shifts one of the electron transfer processes from the solution to the electrode surface, which improves the overall electron transfer, reduces the amount of TEMPO used, and prevents the crossover of this mediator to the anode compartment. We prepared a new TEMPO-pyrrole monomer and deposited an acid-stable conductive polymer using this monomer. The catalytic system consisting of the electrode modified with this polymer and a solution of a  $\text{NO}_x$  mediator system showed activity towards the ORR in an acidic medium.

## 2. Results and Discussion

### 2.1. Synthesis of the TEMPO-Containing Polymer

Existing TEMPO-pyrroles and polymers obtained thereof are based on an ester linker [36–38], which is acid-labile and cannot be utilized in acidic ORR systems. To overcome this issue, we prepared the new TEMPO-pyrrole  $\text{PyC}_4\text{NO}$  with an acid-stable alkyl linker. The  $\text{PyC}_4\text{NO}$  monomer was obtained in two steps (Figure 2). Briefly, TEMPO was alkylated with an excess of 1,4-dibromobutane according to the literature to obtain product **1**, which was then used for the N-alkylation of pyrrole. The alkylation with KOH under typical conditions failed, but the alkylation with NaH as the base yielded the desired monomer  $\text{PyC}_4\text{NO}$ , with a 63% yield.

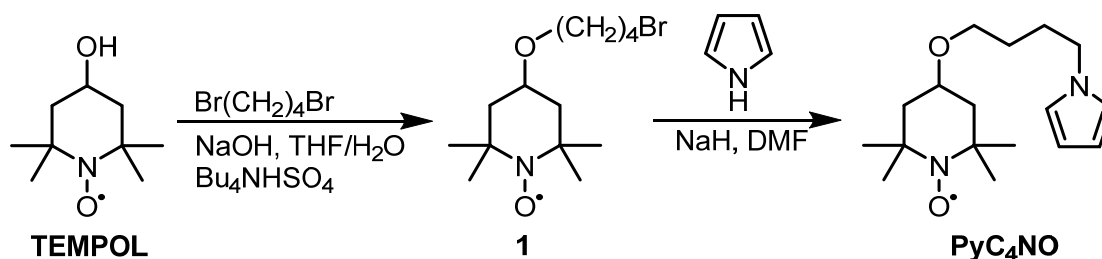
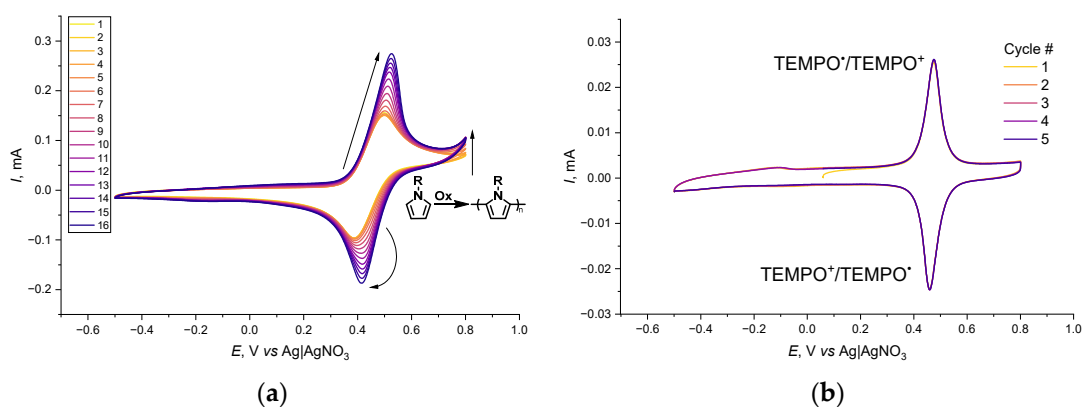


Figure 2. Scheme for the synthesis of  $\text{PyC}_4\text{NO}$ .

Films of *poly*- $\text{PyC}_4\text{NO}$  were deposited via an oxidative electrochemical polymerization of  $\text{PyC}_4\text{NO}$  on the surface of the GC electrode in CV mode (Figure 3a). The irreversible current near an anodic boundary of the CV was attributed to pyrrole oxidation, and the cycle-to-cycle current increase of the peak pair indicated the polymerization of pyrrole  $\text{PyC}_4\text{NO}$  and film growth. A feature worth mentioning is that polymerization reproducibility was scarcely achievable by repeating the vertex potentials, scan rate, and number of CV cycles. The  $\text{PyC}_4\text{NO}$  polymerization process was strongly dependent on slight variations in the electrode potential and the previous history of the solution. To adjust the upper vertex potential accurately, the potential of the TEMPO oxidation of the monomer was used.

As seen in the SEM images of the obtained film (Figure 4), *poly*- $\text{PyC}_4\text{NO}$  appeared as a discontinuous coating consisting of globules with a diameter up to 200 nm. The globules formed a tuberous, but dense layer on the electrode surface.



**Figure 3.** CV curves for the (a) deposition of *poly*-PyC<sub>4</sub>NO from the electrolyte containing 1 mM PyC<sub>4</sub>NO and (b) cycling of *poly*-PyC<sub>4</sub>NO with IR compensation applied; 50 mV s<sup>-1</sup>, 0.1 M Et<sub>4</sub>NBF<sub>4</sub> in CH<sub>3</sub>CN.

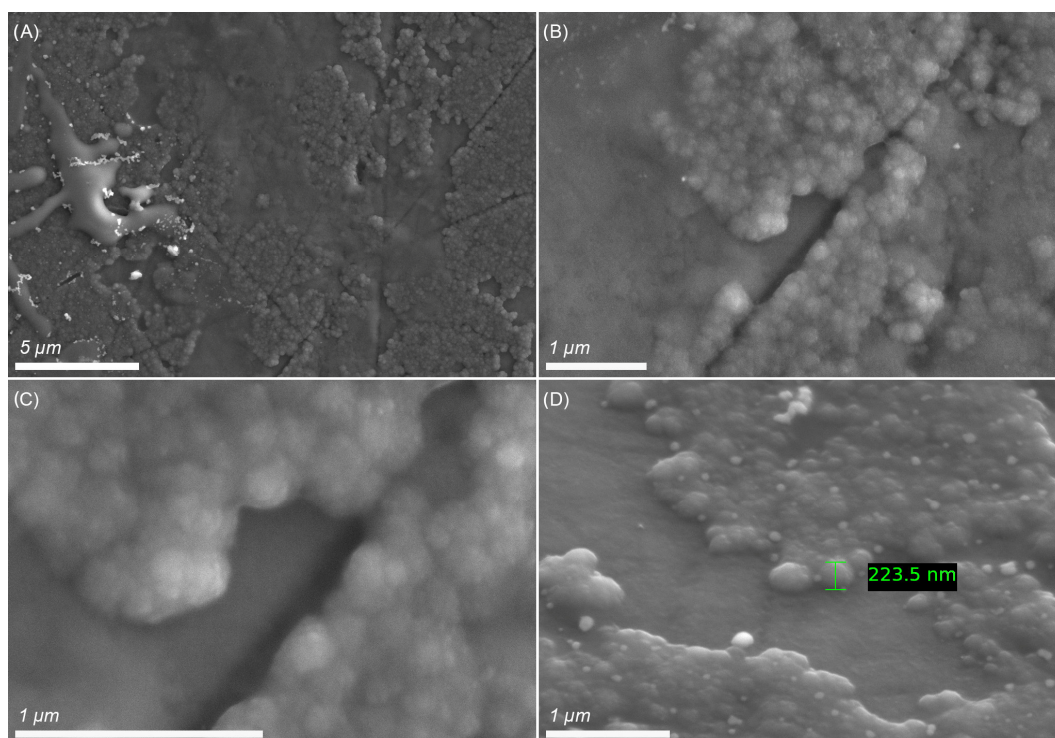


**Figure 4.** SEM images of the *poly*-PyC<sub>4</sub>NO film at different magnifications.

The resulting polymer formed a visible film on the electrode, insoluble in a polymer-free electrolyte, which confirmed the deposition of the polymer. The electrodes obtained were used to study the electrochemical properties of *poly*-PyC<sub>4</sub>NO.

## 2.2. Electrochemical Properties of the Poly-PyC<sub>4</sub>NO-Modified Electrode

The CV spectrum of the freshly deposited film in a neutral electrolyte (Figure 3b) under anaerobic conditions contained a pronounced pair of peaks corresponding to the aminoxyl-oxoammonium one-electron process at 0.47 V. The low peak potential difference (16 mV) indicated the reversibility of this redox process and a fast electron transfer in the film, which acted as a thin layer system without internal diffusion limitations [39,40]. The electrochemical response of the film was stabilized in the second cycle, and no evolution or degradation occurred in the subsequent cycles.

Upon addition of trifluoroacetic acid (TFA) to the electrolyte, the electrochemical response of the *poly*-PyC<sub>4</sub>NO film under anaerobic conditions changed drastically (Figure 5a). In acidic conditions, the TEMPO• particles underwent a proton-coupled disproportionation, affording equal amounts of the corresponding hydroxylamine TEMPOH and oxoammonium cation TEMPO<sup>+</sup> (Figure 5c). Accordingly, from the first CV cycle after the addition of TFA, the currents of the peak pair near 0.45 V dropped rapidly. The TEMPO• fragments underwent disproportionation to TEMPO<sup>+</sup> and TEMPOH (despite the low reduction potential, the latter has a very sluggish oxidation kinetics), resulting in the decrease of the oxidation peak linked to the oxidation of TEMPO• to TEMPO<sup>+</sup>. The resulting TEMPO<sup>+</sup>, being reduced on the backward scan of the CV, disproportionated simultaneously, and the net result of this process was the complete reduction of the TEMPO fragments to TEMPOH. As a result, all TEMPO fragments were brought to the TEMPOH state, which resulted in the disappearance of the peaks of the TEMPO<sup>+</sup>/TEMPO• pair. This process was fully reversible and, when transferred back to the acid-free electrolyte, the electrode restored its electrochemical activity.

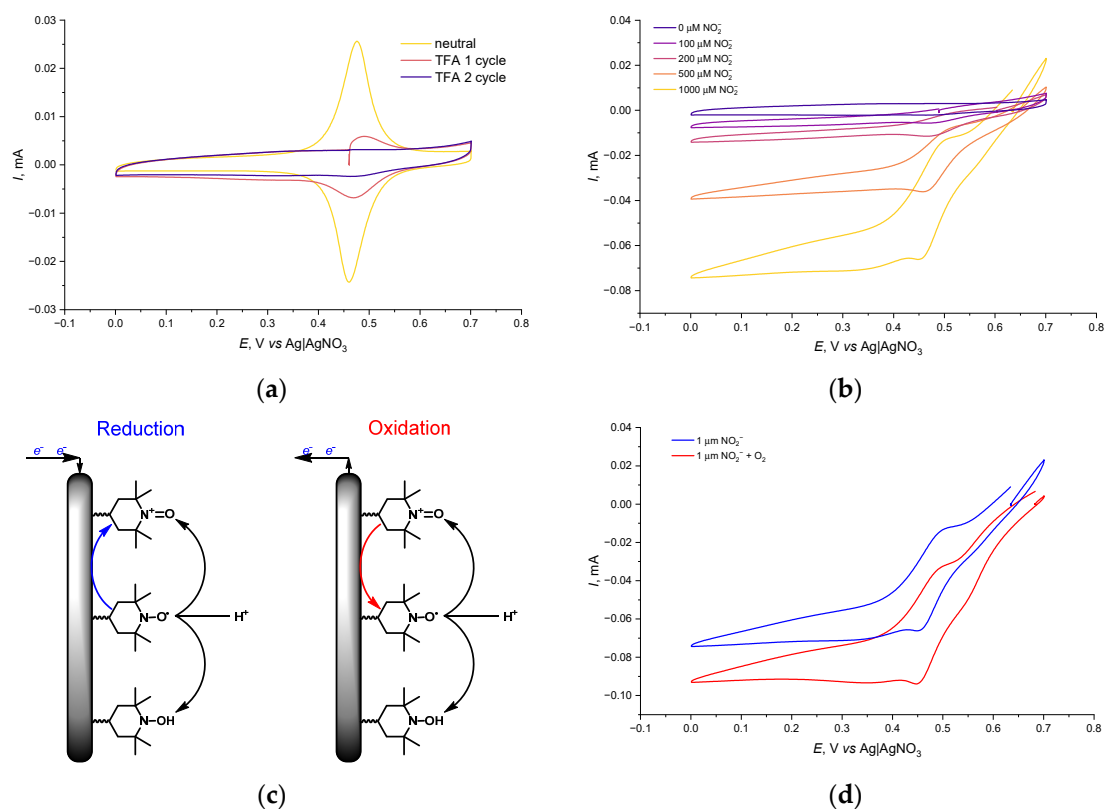


**Figure 5.** CV curves of *poly*-PyC<sub>4</sub>NO (a) in a neutral electrolyte with 0.1 M TFA and (b) in 0.1 M TFA with Bu<sub>4</sub>NNO<sub>2</sub> additives; (c) electrode processes of the TEMPO-containing polymer in an acidic electrolyte and (d) CV curves of *poly*-PyC<sub>4</sub>NO in anaerobic and aerobic conditions, 1 mM Bu<sub>4</sub>NNO<sub>2</sub>, 0.1 M TFA; 50 mV s<sup>-1</sup>, 0.1 M Et<sub>4</sub>NBF<sub>4</sub> in CH<sub>3</sub>CN.

The gradual addition of Bu<sub>4</sub>NNO<sub>2</sub> to the acidified electrolyte under anaerobic conditions resulted in an irreversible cathodic current (Figure 5b), which indicated a fast reduction of NO<sub>2</sub> species on the TEMPO-modified electrode. The cathodic current increased proportionally to the concentration of NO<sub>2</sub><sup>-</sup> up to 1 mM concentration.

In the presence of O<sub>2</sub>, an additional growth of the cathodic current was observed (Figure 5d), which means that some NO<sub>2</sub> reduced on the TEMPO-modified electrode was instantly oxidized back to NO<sub>2</sub> and then brought back to the reaction with a reduced form of TEMPO, according to the proposed double mediator scheme (Figure 1b). Thus, the proposed mediator/catalyst system facilitated the electrochemical reduction of O<sub>2</sub>. Encour-

aged by the performance of the developed system, we decided to study its performance in the ORR in bulk.

### 2.3. Bulk ORR Performance of the Catalytic System

The electrocatalytic properties of the *poly*-PyC<sub>4</sub>NO film were studied by potentiostatic electrolysis at the formal potential of the aminoxy-oxoammonium process, 0.47 V, vs. Ag|AgNO<sub>3</sub> (Figure 6a). As seen from the chronoamperograms, the reduction current in the presence of an oxygen flow became higher after about 10% of electrolysis time, which indicated the depletion of the solution containing NO<sub>2</sub> in the absence of oxygen and its regeneration in the presence of oxygen.

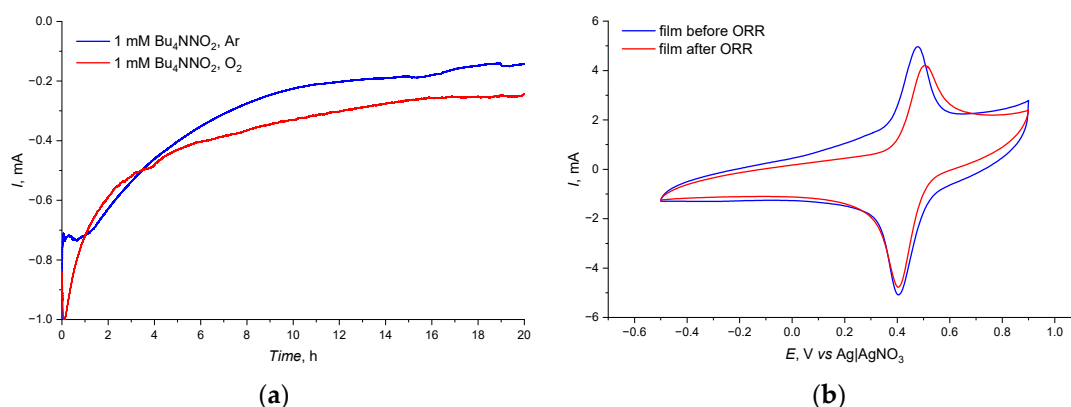


**Figure 6.** (a) Potentiostatic chronoamperogram with and without O<sub>2</sub> on a carbon paper electrode coated with the *poly*-PyC<sub>4</sub>NO film at 0.47 V vs. Ag|AgNO<sub>3</sub>, 1 mM Bu<sub>4</sub>NNO<sub>2</sub> + 0.1 M TFA and (b) CV curve of *poly*-PyC<sub>4</sub>NO before and after the ORR experiments, 50 mV s<sup>-1</sup>; 0.1 M Et<sub>4</sub>NBF<sub>4</sub> in CH<sub>3</sub>CN.

As seen from the CV curve of the *poly*-PyC<sub>4</sub>NO film recorded in an initial electrolyte after the ORR experiments (Figure 6b), the film recovered its electroactivity with only a minor decrease in current, which indicated a high stability of the film under ORR conditions.

## 3. Materials and Methods

**General considerations.** The <sup>1</sup>H and <sup>13</sup>C NMR spectra were recorded on a Bruker Avance 400 spectrometer at 400 and 101 MHz, respectively, in CDCl<sub>3</sub>. Pentafluorophenylhydrazine-d<sub>3</sub> was used to quench the TEMPO radical in situ prior to acquiring the spectrum. ESI-HRMS was recorded using a Shimadzu LCMS-9030 spectrometer in positive mode. SEM was performed on a Zeiss Merlin microscope with a GEMINI II column at 5 kV accelerating voltage in secondary electron mode. The electrochemical experiments were performed on a BioLogic VMP-3e potentiostat.

Starting materials, reagents, and solvents of reagent grade were used as received. The compounds 4-bromobutoxyTEMPO (**1**) [41] and Bu<sub>4</sub>NNO<sub>2</sub> [42] were prepared according to literature protocols. The dry DMF was prepared by fraction distillation from CaH<sub>2</sub> in vacuo. Petroleum ether was dried by storage over activated silica. Electrochemical-grade CH<sub>3</sub>CN and Et<sub>4</sub>NBF<sub>4</sub> were used for the electrochemical experiments. HPLC was performed on an ECOM TOY18DAD800 chromatograph equipped with a YMC 5 μm SiO<sub>2</sub> column; TLC were performed on Merck 60 M F254 indicator silica gel plates.

**Synthesis of PyC<sub>4</sub>NO.** NaH (60% dispersion in mineral oil, 9.25 mmol, 370 mg) was placed in a 30 mL screw cap vial with septum under Ar, washed twice with dry petroleum ether, and dried in vacuo. Dry DMF (6 mL) was injected in the vial under Ar, the reaction mixture was cooled with ice, and then a solution of 1H-pyrrole (5 mmol, 335 mg, 346 μL) in dry DMF (1 mL) was added dropwise via a syringe. After the hydrogen evolution ceased, a solution of **1** (7.25 mmol, 2.27 g) in dry DMF (6 mL) was added dropwise via a syringe. The reaction mixture was stirred at RT for 18 h, quenched with 25 mL of H<sub>2</sub>O, and diluted with 30 mL of CH<sub>2</sub>Cl<sub>2</sub>. The organic layer was separated, thoroughly washed with brine

3 times, dried over  $\text{Na}_2\text{SO}_4$ , and the solvent was removed in vacuo. The crude product was purified by preparative HPLC (silica gel, hexane–acetone gradient), giving the desired product, an orange solid with a yield of 63% (922 mg).

$\text{PyC}_4\text{NO}$ :  $^1\text{H}$  NMR ( $\text{CDCl}_3$ , 400 MHz)  $\delta$  (ppm) 6.67 (t,  $J = 2$  Hz, 2H), 6.15 (t,  $J = 2$  Hz, 2H), 3.93 (t,  $J = 7.1$  Hz, 2H), 3.61–3.49 (m, 1H), 3.44 (t,  $J = 6.3$  Hz, 2H), 2.06–1.74 (m, 4H), 1.68–1.51 (m, 2H), 1.51–1.38 (m, 2H), 1.23 (s, 6H), 1.17 (s, 6H);  $^{13}\text{C}$  NMR ( $\text{CDCl}_3$ , 101 MHz)  $\delta$  (ppm) 120.5, 107.9, 70.5, 67.6, 59.2, 49.5, 44.8, 32.0, 28.6, 27.4, 20.7; ESI HRMS  $m/z$  [ $\text{M}$ ] $^+$  calcd for  $\text{C}_{17}\text{H}_{29}\text{N}_2\text{O}_2^+$  293.2224, found 293.2226.

**Electrochemical experiments.** Poly- $\text{PyC}_4\text{NO}$  films were deposited onto the prepared glassy carbon (GC) electrodes ( $d = 3$  mm) by oxidative electrochemical polymerization of  $\text{PyC}_4\text{NO}$  from its 1 mM solution in  $\text{CH}_3\text{CN}$  containing 0.1 M  $\text{Et}_4\text{NBF}_4$  as a supporting electrolyte. The preparation of the GC electrode included subsequent polishing, rinsing with isopropyl alcohol and acetone, drying and electrochemical pretreatment procedures (application of constant potentials of 1.5,  $-1.0$ , 1.5,  $-1.0$  V vs. an  $\text{Ag}|\text{AgNO}_3$  reference electrode for 2 min in 0.1 M  $\text{Et}_4\text{NBF}_4$ ,  $\text{CH}_3\text{CN}$  electrolyte). Polymerization was carried out in a standard three-electrode cell equipped with a Pt strip as an auxiliary electrode and a BASi MW-1085  $\text{Ag}|\text{AgNO}_3$  non-aqueous reference electrode. Polymerization was carried out in the cyclic voltammetry (CV) mode in the range of  $-0.5$ – $0.8$  V with a scan rate of 50 mV for 16 cycles. After the deposition, the obtained films were washed with  $\text{CH}_3\text{CN}$  and dried in air.

For the potentiostatic experiments, poly- $\text{PyC}_4\text{NO}$  films were deposited onto a carbon paper disc electrode ( $d = 16$  mm) following the same procedure as described above, but with the electrode pre-treatment step omitted. Potentiostatic electrolysis was performed in a three-electrode cell with a glass frit dividing the working and the counter electrode compartments. The solution volume in the working electrode compartment was 25 mL. Before electrolysis, the solution was purged with argon or oxygen, and electrolysis was performed in a sealed cell under static pressure of the desired gas.

#### 4. Conclusions

The immobilization of TEMPO-groups on the electrode surface by help of a conductive polymer backbone is an effective way to utilize the catalytic properties of the TEMPO radical in heterogeneous catalytic cycles. In this work, we demonstrated an efficient ORR cycle consisting of dissolved  $\text{NO}_x$  and an electrode modified with a TEMPO-containing polymer. The former one provided a facile  $\text{O}_2$  reduction, while the latter one boosted the electron transfer from the electrode surface. The TEMPO-containing polymer was easily deposited directly on the electrode surface by an electrochemical polymerization. Immobilization of TEMPO on the electrode surface allowed us to reduce the amount of the TEMPO-containing catalyst with respect to that of the dissolved  $\text{NO}_x$  mediator system and prevent the possible crossover of TEMPO species. Because of the high potential of both redox processes involved in the proposed cycle, this system preserved most of the energy of the ORR half-reaction. This system may be further employed in proton-exchange fuel cells. Since this system is able to operate under nonaqueous conditions, it can be exploited at temperatures below  $0^\circ\text{C}$ , which is beneficial for transport and, in general, outdoor applications.

**Author Contributions:** Conceptualization, D.A.L. and O.V.L.; methodology, D.A.L., A.Y.K. and O.V.L.; validation, A.Y.K., O.Y.B., V.V.P. and L.G.R.; investigation, A.Y.K. and L.G.R.; resources, O.V.L.; data curation, A.Y.K.; writing—original draft preparation, D.A.L.; writing—review and editing, O.V.L.; supervision, O.V.L.; funding acquisition, O.V.L. All authors have read and agreed to the published version of the manuscript.

**Funding:** The reported study was funded by RFBR, Sirius University of Science and Technology, JSC Russian Railways and Educational Fund “Talent and success”, project number 20-33-51007.

**Data Availability Statement:** The data presented in this study are available on request from the corresponding author.

**Acknowledgments:** We thank the Research Center for Magnetic Resonance, the Center for Chemical Analysis and Materials Research, the Interdisciplinary Resource Centre for Nanotechnology, and the Centre for Extreme States of Materials and Constructions of Saint Petersburg State University Research Park for the measurements and fabrication processes.

**Conflicts of Interest:** The authors declare no conflict of interest. The funders had no role in the design of the study; in the collection, analyses, or interpretation of data; in the writing of the manuscript; or in the decision to publish the results.

## References

1. Shao, M.; Chang, Q.; Dodelet, J.P.; Chenitz, R. Recent Advances in Electrocatalysts for Oxygen Reduction Reaction. *Chem. Rev.* **2016**, *116*, 3594–3657. [[CrossRef](#)] [[PubMed](#)]
2. Suermann, M.; Schmidt, T.J.; Büchi, F.N. Comparing the kinetic activation energy of the oxygen evolution and reduction reactions. *Electrochim. Acta* **2018**, *281*, 466–471. [[CrossRef](#)]
3. Kulkarni, A.; Siahrostami, S.; Patel, A.; Norskov, J.K. Understanding Catalytic Activity Trends in the Oxygen Reduction Reaction. *Chem. Rev.* **2018**, *118*, 2302–2312. [[CrossRef](#)] [[PubMed](#)]
4. Mase, K.; Ohkubo, K.; Fukuzumi, S. Efficient two-electron reduction of dioxygen to hydrogen peroxide with one-electron reductants with a small overpotential catalyzed by a cobalt chlorin complex. *J. Am. Chem. Soc.* **2013**, *135*, 2800–2808. [[CrossRef](#)] [[PubMed](#)]
5. Baran, J.D.; Gronbeck, H.; Hellman, A. Analysis of porphyrines as catalysts for electrochemical reduction of O<sub>2</sub> and oxidation of H<sub>2</sub>O. *J. Am. Chem. Soc.* **2014**, *136*, 1320–1326. [[CrossRef](#)]
6. Inaba, M.; Yamada, H.; Tokunaga, J.; Matsuzawa, K.; Hatanaka, A.; Tasaka, A. Hydrogen Peroxide Formation as a Degradation Factor of Polymer Electrolyte Fuel Cells. *ECS Trans.* **2006**, *1*, 315–322. [[CrossRef](#)]
7. Huang, L.; Zaman, S.; Tian, X.; Wang, Z.; Fang, W.; Xia, B.Y. Advanced Platinum-Based Oxygen Reduction Electrocatalysts for Fuel Cells. *Acc. Chem. Res.* **2021**, *54*, 311–322. [[CrossRef](#)]
8. Sui, S.; Wang, X.; Zhou, X.; Su, Y.; Riffat, S.; Liu, C.-J. A comprehensive review of Pt electrocatalysts for the oxygen reduction reaction: Nanostructure, activity, mechanism and carbon support in PEM fuel cells. *J. Mater. Chem. A* **2017**, *5*, 1808–1825. [[CrossRef](#)]
9. Winter, M.; Brodd, R.J. What Are Batteries, Fuel Cells, and Supercapacitors? *Chem. Rev.* **2004**, *104*, 4245–4270. [[CrossRef](#)]
10. Gewirth, A.A.; Varnell, J.A.; DiAscro, A.M. Nonprecious Metal Catalysts for Oxygen Reduction in Heterogeneous Aqueous Systems. *Chem. Rev.* **2018**, *118*, 2313–2339. [[CrossRef](#)]
11. Cui, J.; Chen, Q.; Li, X.; Zhang, S. Recent advances in non-precious metal electrocatalysts for oxygen reduction in acidic media and PEMFCs: An activity, stability and mechanism study. *Green Chem.* **2021**, *23*, 6898–6925. [[CrossRef](#)]
12. Shahbaz, A.; Afaf, A.; Tahir, N.; Abid, U.; Saim, S. Non Precious Metal Catalysts: A Fuel Cell and ORR Study of Thermally Synthesized Nickel and Platinum Mixed Nickel Nanotubes for PEMFC. *Key Eng. Mater.* **2021**, *875*, 193–199. [[CrossRef](#)]
13. Zhang, J.; Sasaki, K.; Sutter, E.; Adzic, R.R. Stabilization of platinum oxygen-reduction electrocatalysts using gold clusters. *Science* **2007**, *315*, 220–222. [[CrossRef](#)] [[PubMed](#)]
14. Iijima, Y.; Kondo, T.; Takahashi, Y.; Bando, Y.; Todoroki, N.; Wadayama, T. Oxygen Reduction Reaction Activities for Pt/Au(hkl) Bimetallic Surfaces Prepared by Molecular Beam Epitaxy. *J. Electrochem. Soc.* **2013**, *160*, F898–F904. [[CrossRef](#)]
15. Chen, G.; Zhao, Y.; Fu, G.; Duchesne, P.N.; Gu, L.; Zheng, Y.; Weng, X.; Chen, M.; Zhang, P.; Pao, C.-W.; et al. Interfacial Effects in Iron-Nickel Hydroxide–Platinum Nanoparticles Enhance Catalytic Oxidation. *Science* **2014**, *344*, 495–499. [[CrossRef](#)] [[PubMed](#)]
16. Wang, C.; Markovic, N.M.; Stamenkovic, V.R. Advanced Platinum Alloy Electrocatalysts for the Oxygen Reduction Reaction. *ACS Catal.* **2012**, *2*, 891–898. [[CrossRef](#)]
17. Qu, L.; Liu, Y.; Baek, J.-B.; Dai, L. Nitrogen-Doped Graphene as Efficient Metal-Free Electrocatalyst for Oxygen Reduction in Fuel Cells. *ACS Nano* **2010**, *4*, 1321–1326. [[CrossRef](#)]
18. Cai, P.W.; Ci, S.Q.; Zhang, E.H.; Shao, P.; Cao, C.S.; Wen, Z.H. FeCo Alloy Nanoparticles Confined in Carbon Layers as High-activity and Robust Cathode Catalyst for Zn-Air Battery. *Electrochim. Acta* **2016**, *220*, 354–362. [[CrossRef](#)]
19. Chai, G.-L.; Boero, M.; Hou, Z.; Terakura, K.; Cheng, W. Indirect Four-Electron Oxygen Reduction Reaction on Carbon Materials Catalysts in Acidic Solutions. *ACS Catal.* **2017**, *7*, 7908–7916. [[CrossRef](#)]
20. Gong, X.; Liu, S.; Ouyang, C.; Strasser, P.; Yang, R. Nitrogen- and Phosphorus-Doped Biocarbon with Enhanced Electrocatalytic Activity for Oxygen Reduction. *ACS Catal.* **2015**, *5*, 920–927. [[CrossRef](#)]
21. Shao, Y.; Jiang, Z.; Zhang, Q.; Guan, J. Progress in Nonmetal-Doped Graphene Electrocatalysts for the Oxygen Reduction Reaction. *ChemSusChem* **2019**, *12*, 2133–2146. [[CrossRef](#)]
22. An, F.; Bao, X.-Q.; Deng, X.-Y.; Ma, Z.-Z.; Wang, X.-G. Carbon-based metal-free oxygen reduction reaction electrocatalysts: Past, present and future. *New Carbon Mater.* **2022**, *37*, 338–354. [[CrossRef](#)]
23. Zheng, Q.; Cheng, X.; Jao, T.-C.; Weng, F.-B.; Su, A.; Chiang, Y.-C. Degradation analyses of Ru85Se15 catalyst layer in proton exchange membrane fuel cells. *J. Power Sources* **2012**, *218*, 79–87. [[CrossRef](#)]
24. Wu, J.; Yuan, X.Z.; Martin, J.J.; Wang, H.; Zhang, J.; Shen, J.; Wu, S.; Merida, W. A review of PEM fuel cell durability: Degradation mechanisms and mitigation strategies. *J. Power Sources* **2008**, *184*, 104–119. [[CrossRef](#)]

25. Elmas, S.; Beelders, W.; Pan, X.; Nann, T. Conducting copper(I/II)-metallopolymer for the electrocatalytic oxygen reduction reaction (ORR) with high kinetic current density. *Polymers* **2018**, *10*, 1002. [[CrossRef](#)]
26. Bratsch, S.G. Standard Electrode Potentials and Temperature Coefficients in Water at 298.15 K. *J. Phys. Chem. Ref. Data* **1989**, *18*, 1–21. [[CrossRef](#)]
27. Gerken, J.B.; Pang, Y.Q.; Lauber, M.B.; Stahl, S.S. Structural Effects on the pH-Dependent Redox Properties of Organic Nitroxyls: Pourbaix Diagrams for TEMPO, ABNO, and Three TEMPO Analogs. *J. Org. Chem.* **2018**, *83*, 7323–7330. [[CrossRef](#)] [[PubMed](#)]
28. Kimura, M.; Sato, M.; Murase, T.; Tsukahara, K. Kinetic Studies of the Reaction of Nitrous Acid with Iodide Ion in the Presence of Molecular Oxygen in an Acid Solution. *Bull. Chem. Soc. Jpn.* **1993**, *66*, 2900–2906. [[CrossRef](#)]
29. Anson, C.W.; Stahl, S.S. Mediated Fuel Cells: Soluble Redox Mediators and Their Applications to Electrochemical Reduction of O<sub>2</sub> and Oxidation of H<sub>2</sub>, Alcohols, Biomass, and Complex Fuels. *Chem. Rev.* **2020**, *120*, 3749–3786. [[CrossRef](#)]
30. Nutting, J.E.; Mao, K.; Stahl, S.S. Iron(III) Nitrate/TEMPO-Catalyzed Aerobic Alcohol Oxidation: Distinguishing between Serial versus Integrated Redox Cooperativity. *J. Am. Chem. Soc.* **2021**, *143*, 10565–10570. [[CrossRef](#)]
31. Ryland, B.L.; Stahl, S.S. Practical aerobic oxidations of alcohols and amines with homogeneous copper/TEMPO and related catalyst systems. *Angew. Chem. Int. Ed. Engl.* **2014**, *53*, 8824–8838. [[CrossRef](#)] [[PubMed](#)]
32. Ford, P.C.; Wink, D.A.; Stanbury, D.M. Autoxidation kinetics of aqueous nitric oxide. *FEBS Lett.* **1993**, *326*, 1–3. [[CrossRef](#)]
33. Kummer, J.T.; Oei, D.G. A chemically regenerative redox fuel cell. II. *J. Appl. Electrochem.* **1985**, *15*, 619–629. [[CrossRef](#)]
34. Bergens, S.H.; Gorman, C.B.; Palmore, G.T.; Whitesides, G.M. A Redox Fuel Cell That Operates with Methane as Fuel at 120 °C. *Science* **1994**, *265*, 1418–1420. [[CrossRef](#)] [[PubMed](#)]
35. Gerken, J.B.; Stahl, S.S. High-Potential Electrocatalytic O<sub>2</sub> Reduction with Nitroxyl/NO<sub>x</sub> Mediators: Implications for Fuel Cells and Aerobic Oxidation Catalysis. *ACS Cent. Sci.* **2015**, *1*, 234–243. [[CrossRef](#)]
36. Xu, L.H.; Yang, F.; Su, C.; Zhang, C. Research of Properties on Li-Ion Batteries Based on a Polypyrrole Derivative Bearing TEMPO as a Cathode Material. *Adv. Mater. Res.* **2014**, *936*, 447–451. [[CrossRef](#)]
37. Xu, L.; Guo, P.; He, H.; Zhou, N.; Ma, J.; Wang, G.; Zhang, C.; Su, C. Preparation of TEMPO-contained pyrrole copolymer by in situ electrochemical polymerization and its electrochemical performances as cathode of lithium ion batteries. *Ionics* **2017**, *23*, 1375–1382. [[CrossRef](#)]
38. Xu, L.; Yang, F.; Su, C.; Ji, L.; Zhang, C. Synthesis and properties of novel TEMPO-contained polypyrrole derivatives as the cathode material of organic radical battery. *Electrochim. Acta* **2014**, *130*, 148–155. [[CrossRef](#)]
39. Malev, V.V.; Levin, O.V. Criteria of the absence of short-range interactions within electroactive polymer films. *Electrochim. Acta* **2012**, *80*, 426–431. [[CrossRef](#)]
40. Laviron, E. Adsorption, Autoinhibition and Autocatalysis in Polarography and in Linear Potential Sweep Voltammetry. *J. Electroanal. Chem.* **1974**, *52*, 355–393. [[CrossRef](#)]
41. Zheng, Z.; Wang, J.; Chen, H.; Feng, L.; Jing, R.; Lu, M.; Hu, B.; Ji, J. Magnetic Superhydrophobic Polymer Nanosphere Cage as a Framework for Micellar Catalysis in Biphasic Media. *ChemCatChem* **2014**, *6*, 1626–1634. [[CrossRef](#)]
42. Bhatt, V.D.; Gohil, K. Ion exchange synthesis and thermal characteristics of some [N+4444] based ionic liquids. *Thermochim. Acta* **2013**, *556*, 23–29. [[CrossRef](#)]